DENSIFICATION AND MICROSTRUCTURE CHARACTERISTICS OF A PREALLOYED ALPHA BRASS POWDER PROCESSED BY LIQUID PHASE SINTERING

A. Mohammadzadeh*,[1], A. Sabahi Namini[2] and M. Azadbeh[1]

* *amzadeh@ymail.com*

Received: May 2014 **Accepted: August 2014**

[1] Department of Materials Engineering, Sahand University of Technology, Tabriz, Iran.

[2] Young Researchers and Elite Club, Ilkhchi Branch, Islamic Azad University, Ilkhchi, Iran.

Abstract: *The rapidly solidified prealloyed alpha brass powder with a size range of 40 to 100 μm produced by water atomization process was consolidated using liquid phase sintering process. The relationships between sintering temperature, physic-mechanical properties and microstructural characteristics were investigated. Maximum densification was obtained at 930 °C, under 600 MPa compacting pressure, with 60 min holding time. The microstructure of the sintered brass was influenced by dezincification and structural coarsening during supersolidus liquid phase sintering. As a consequence of Kirkendall effect atomic motion between Cu and Zn atoms caused to dezincification at the grain boundaries and formation of ZnO particles on the pore surfaces. It was concluded that microstructural analysis is in a well agreement with obtained physical and mechanical properties. Also, the amount of liquid phase, which depends on sintering temperature, results in different load bearing cross section areas, and it affects the type of fracture morphologies.*

Keywords: *Cu-20Zn alloy, Supersolidus liquid phase sintering, Densification and Coarsening.*

1. INTRODUCTION

Alpha brass alloys are widely used as an industrial material because of their excellent characteristics such as high corrosion resistance, diamagnetism, good deformability and machinability [1-3]. Basic applications in automotive industries for brass powder metallurgy (PM) parts include bearings and synchronizer rings. Generally sintered brass parts are commonly made from prealloyed atomized powders [4]. These parts are pressed by various methods. Cold pressing of brass powders, giving green densities of 7.3 – 7.6 $g.cm^{-3}$ at pressures of 600-800 MPa, is one of the most common methods [4, 5]. Sintering of brass is normally performed in a temperature range from 815 to 925 °C depending on the alloy composition.

The sintering process of brass components made from prealloyed powders includes liquid phase formation, most effectively evolves supersolidus liquid phase sintering (SLPS), where liquid forms when the material is heated just beyond the solidus temperature. The commonly observed liquid formation sites are the grain boundaries within particles, the interparticle neck region and the grain interior. These sites depend on several factors, such as powder microstructure, alloy chemistry, particle size, and the heating rate. Formed internal liquid spreads along the grain boundaries to create an interparticle capillary bond that induces densification during sintering [6-10]. Densification of brass during sintering by SLPS is sensitive to temperature. So temperature control plays the most important role during SLPS. As the liquid volume fraction increases, at a critical temperature above the solidus, a threshold amount of liquid exists along the grain boundaries. Sintering below a threshold temperature results in incomplete densification due to insufficient liquid. The upper critical temperature is dictated by the shape distortion that results from the presence of excess liquid. To avoid distortion or blistering of the compacts, sintering temperatures should not exceed the critical temperature of the alloy [11-13].

The present study investigates the sintering response of Cu-20Zn alloy that has been consolidated through SLPS and evaluates its densification, microstructure and mechanical properties. Effect of heating mode has been investigated as a function of sintering temperature. Scanning electron microscopy

(SEM) and energy dispersive x-ray spectroscopy (EDS) have been conducted to study fracture analysis and chemical characterization.

2. MATERIALS AND METHODS

Water atomized prealloyed Cu-20Zn powder with particle size of 40 to 100 μm (particle fraction obtained by sieving method according to ASTM E11 standard) provided by Tabriz Powder Metallurgy Company was used as the base material. After characterization of the flow behavior (based on ASTM B213) and apparent density (based on ASTM B212), the brass powder was mixed with 0.75 wt% lithium stearate as lubricant in a V shaped mixer at 65 rpm for a period of 60 min. The obtained powder mixture, used as the base material for all specimens, was compacted into Charpy bars of 55 mm × 10 mm × 10 mm using a pressure of 600 MPa in a uniaxial hydraulic press, using a tool with floating die. The green density was calculated by measuring the compact weight and dimensions. To avoid the compacts sticking together during sintering and to reduce Zn evaporation, the compacts were placed in a ceramic boat filled with alumina powder. The heating cycle included a 30 min dwell in the dewaxing zone at 540 °C for delubrication followed by sintering in the high temperature zone at different temperatures between 900 to 950°C for 60 min in a small laboratory furnace (type, TFS/25-1250). An Ar flow of 2 l/min was maintained throughout the entire cycle. Sintered compacts was left in the exit zone for natural cooling. The sintered specimens were characterized by measuring the density through water displacement. In this case the density was determined by the Archimedes method (DIN ISO 3369).

The length of green and sintered compacts was determined by a caliper with 0.02 mm precision, and the dimensional changes were calculated. The apparent hardness of the sintered parts was determined by ESWAY vickers hardness tester at 30 kgf load. The recorded hardness values are the average of six readings taken at random spots throughout the metallographic sections. Impact energy was measured using a 300 J Charpy impact tester (type, "ROELL AMSLER") according to ASTM En23-01 standard. The sintered specimens were sectioned in parallel to the pressing direction, polished and etched (8 g $FeCl_3$, 25 ml HCl, 50 ml H_2O). Microstructural examination of the etched specimens was conducted using an optical microscope (OM) and CAM SCAN 2300 scanning electron microscope (SEM). Fractographic investigation and chemical analysis of the fracture surfaces of impact test samples were performed using the SEM equipped with an energy dispersive x-ray spectroscope (EDS).

3. RESULTS AND DISCUSSION

3. 1. Powder Characteristics

The composition and SEM micrograph of the raw powder are shown in Table 1. The particles showed an irregular shape with a mean size of 40 to 100 μm. According to chemical composition the amount of Zn content is about 20.5 wt. % which it is an alpha brass that contains one phase with a face-centered cubic crystal structure.

3. 2. Sintering Characteristics

The variation in sintered density with sintering temperature at different temperatures (900–950°C) is shown in Fig. 1 (a). It can be seen from sintering curve that sintered densities decrease gradually after the optimum sintering temperature at 930 °C, but increase more rapidly before this temperature. Fig. 1 (b) also shows that hardness and impact energy increase as the sintering temperature increases from 900 to 930 °C with a similar trend for the sintered density. Therefore, the results reveal that the optimum sintering condition is at a temperature of 930 °C for 60 min. The changes in length of the sintered samples are shown in Fig. 1 (a). The response of dimensional change to sintering temperature is in a good agreement to that of the sintered density. Accordingly, up to 930 °C there is a significant shrinkage (about 3.43%) of the sintered compact compared to the green one, while at 940 and 950°C shrinkage is lower.

Table 1. Morphology and characteristics of the used brass powder.

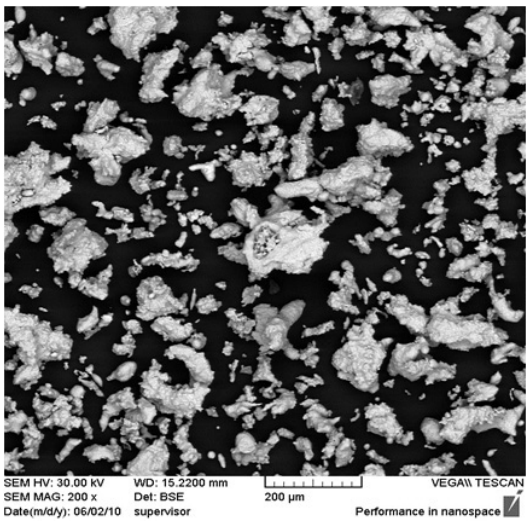

Brass powder properties	
Apparent density (g/cm³)	3.2
Flowability (sec/50g)	28
Powder shape	Irregular
Chemical analysis	
Zn (wt. %)	20.5
Pb (wt. %)	0.52
Sn (wt. %)	0.4
Al-Fe-Ni (wt. %)	< 0.5
Cu (wt. %)	Balance

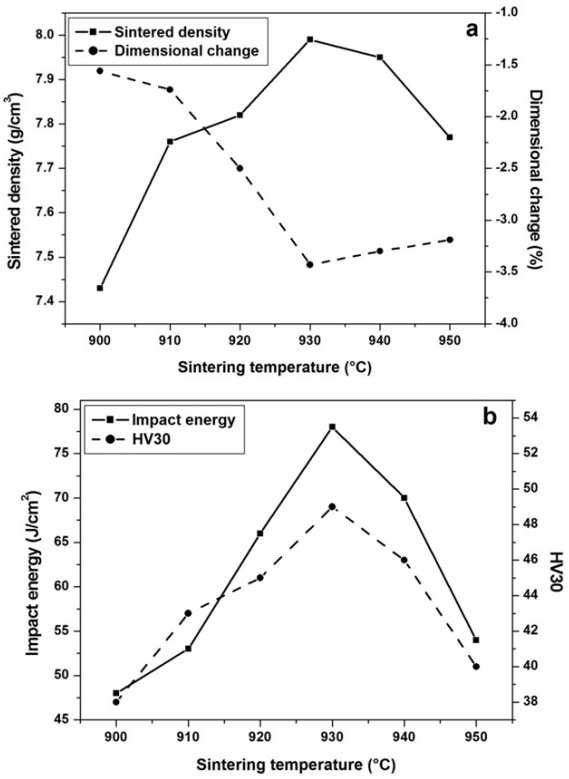

Fig. 1. The effect of sintering temperature on properties of sintered Cu-20Zn; (a) sintered density and dimensional change, and (b) impact energy and hardness.

3. 3. Microstructural Analysis

3. 3. 1. Metallographic Observations

Based on the microstructural features, which presented in Fig. 2, grain growth and pore coarsening were distinguished in the microstructure of sintered samples. As the used powder is prealloyed, the sintering process is of SLPS type, the schematic stages of which are shown in Fig. 3. By increasing the sintering temperature to a level between solidus and liquidus (Fig. 3), the amount of formed liquid is augmented and so fragmentation and rearrangement of grains is developed.

In the effect of increasing sintering temperature, rearrangement of grains from fragmented powder particles as a result of further liquid phase formation leads to higher densification and sphericity of grains. In spite of decreasing pore number, pore coarsening and grain growth occur concurrently with shape accommodation so that small grains are dissolved and reprecipitated on large grains through Ostwald ripening or grain coalescence. After sintering above 930 °C, the growth of grains and pores can be a good reason for a decrease in sintered density and impact energy. Regarding the lower pore number: increasing sintering

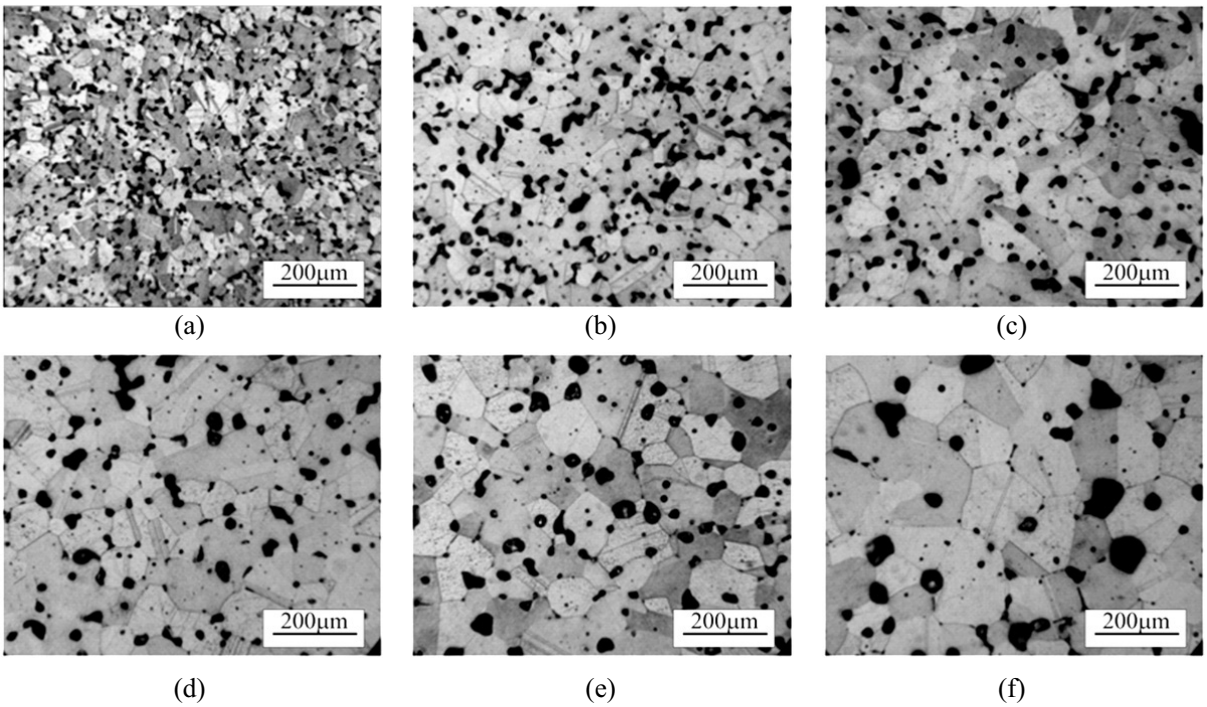

Fig. 2. Microstructure of brass compacts sintered at different temperatures for 60 min in Ar atmosphere; (a) 900 °C, (b) 910 °C, (c) 920 °C, (d) 930 °C, (e) 940 °C, (f) 950 °C.

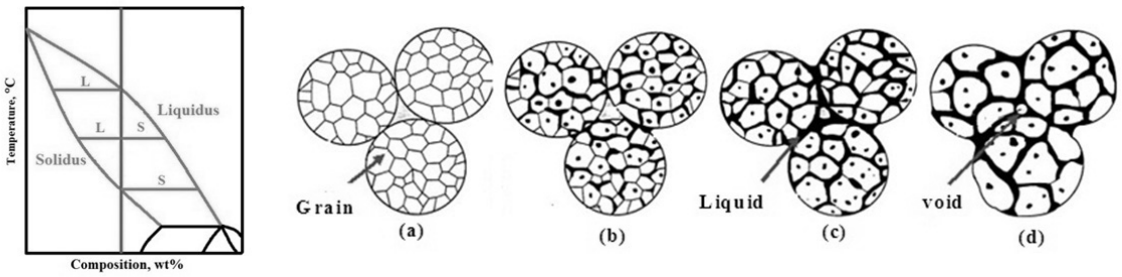

Fig. 3. Schematic stages of supersolidus sintering processes in a narrow temperature window between solidus and liquidus, (a) initial particle packing, (b) formation of initial liquid with insufficient penetration of grain boundaries for densification, (c) viscous flow densification of semisolid particles, (d) final stage densification with closed, spherical pores [9].

temperature can be positive because of more sliding and grain repacking and more interfacial bonding. Considering however the structural coarsening, increasing sintering temperature has a negative effect. Between these two antithetical extreme effects there is an optimum state to achieve the highest density as a sound basis to obtain improved mechanical properties.

3. 3. 2. Fractographic Observations

The scanning electron microscopy of the brass sample is shown in Fig. 4. The pores at all regions of the sintered compact at 910 °C are distributed non-uniform and are small in size. In addition, fracture occurs at the grain boundary regions, where the initial liquid phase forms, and apparently no transgranular fracture is observed.

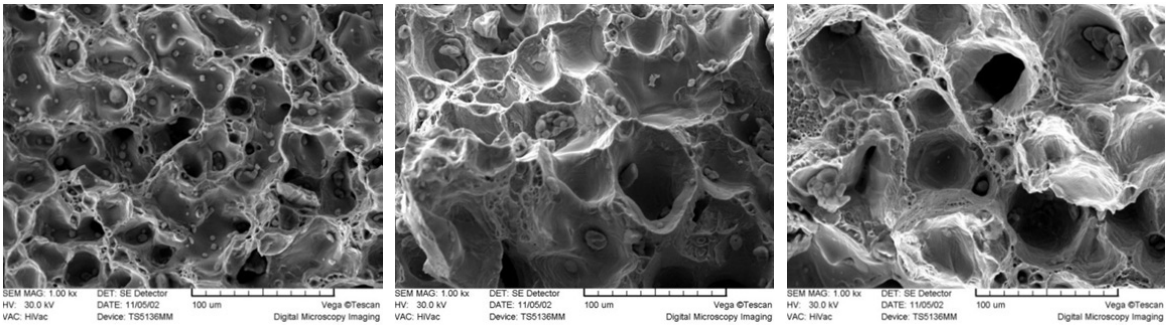

(a) (b) (c)

Fig. 4. Fracture surface of specimens sintered at different temperatures for 60 min in Ar atmosphere followed by cooling in exit zone of furnace: (a) 910 °C, (b) 930 °C, (c) 950 °C.

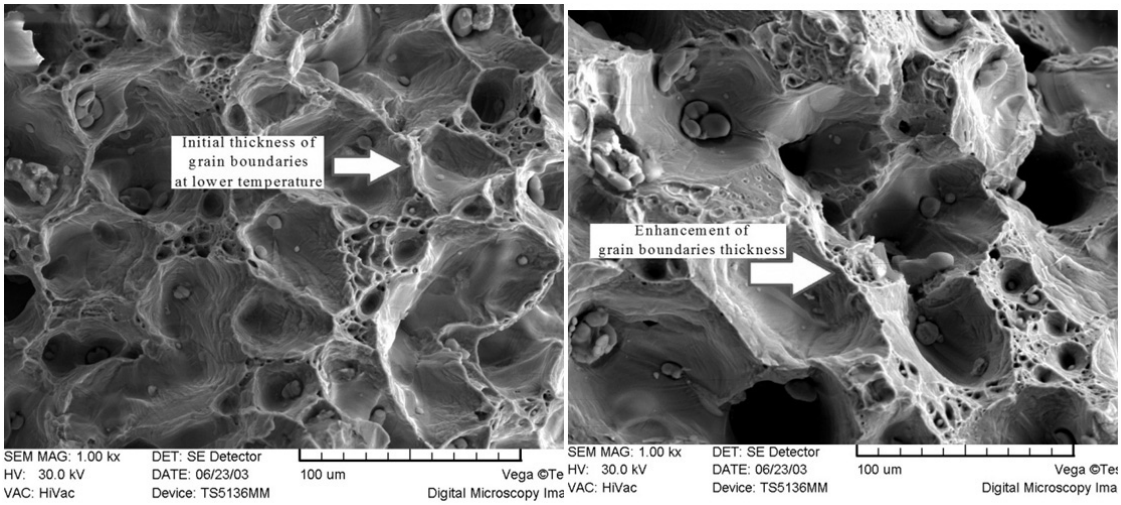

Sintering temperature = 930 °C Sintering temperature = 950 °C

Fig. 5. Thickness of the accumulated secondary phase in the grain boundaries.

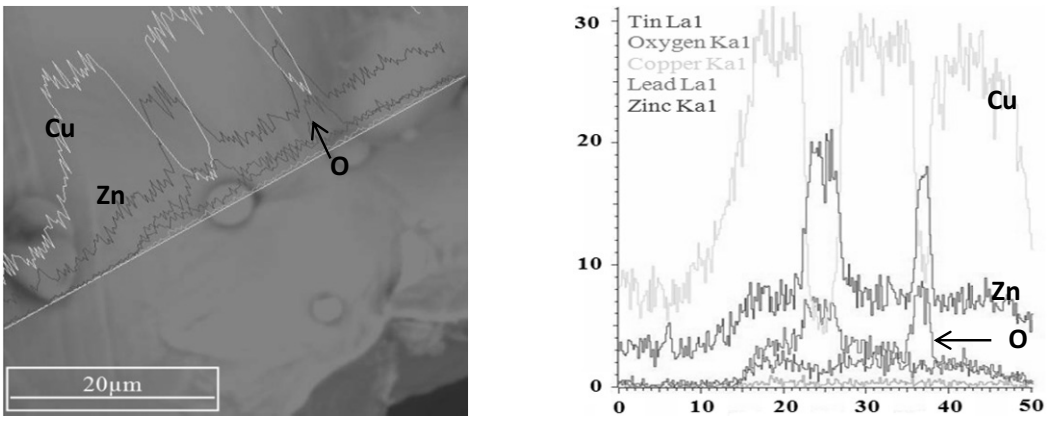

(a) (b)

Fig. 6. Linear and map analysis images of Zn and Pb distribution in the cross section of sintered sample at 930 °C; (a) Image of fracture surface and (b) elements contents.

Increasing the temperature caused to pore filing and pore coarsening from 930 to 950 °C.

Thickness of the accumulated liquid phase in the grain boundaries of the fractured brass component is depicted in Fig. 5. Grain growth, and consequently pore coarsening at 950 °C occur more than other temperatures. Hence, with increasing liquid phase at 950 °C, thickness of the accumulated phase in the grain boundaries is enhanced (Fig. 5).

According to the fracture surfaces some droplets can be observed at the grain boundaries and pores surfaces. An EDS taken in a representative area of sintered sample at 930 °C (Fig. 6), which indicates that the amount of oxygen at the grain boundary is increased along with the zinc content. It can be concluded that these droplets are zinc oxides.

To investigate the changes in chemical composition caused by liquid phase formation in a pore interior, also a linear analysis was done on the pore interior surface of the sintered compact

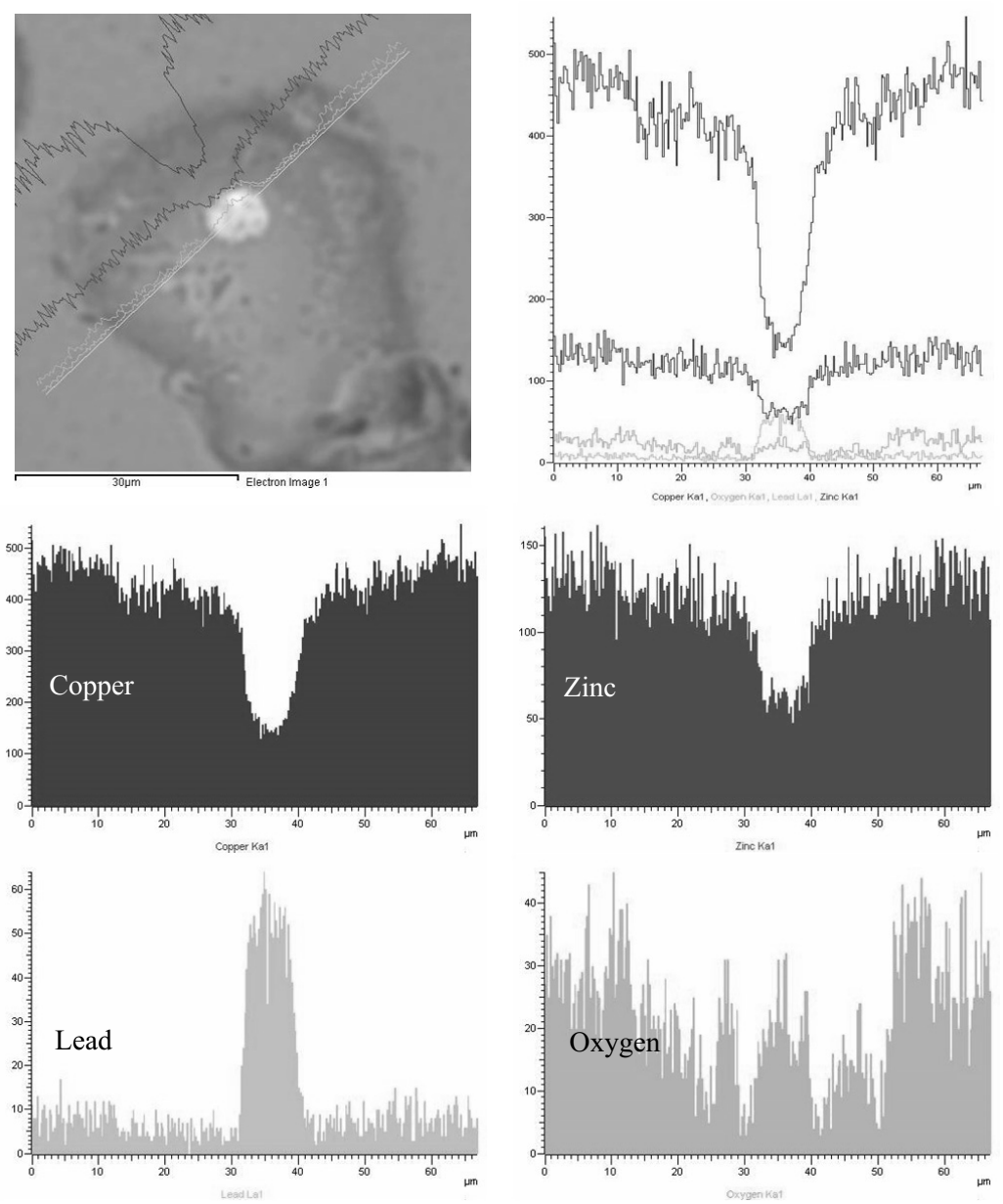

Fig. 7. Line scan analysis from a pore interior that shows Pb segregation.

at 930 °C (Fig. 7). The difference in the chemical composition of white droplet and pore surface is clear, so that the amount of Cu and Zn at the droplet location decreased. Such a change in chemical composition could be responsible for the lower wettability of Pb that segregated and remained in the pore surface.

In general two kind of segregated particles are present in the fracture surfaces of the sintered Cu-20Zn that was proved by EDS. ZnO could be formed as a result of Kirkendall effect and Zn redistribution, while Pb because of the lower surface energy segregated like white particles on the pore surfaces.

4. CONCLUSIONS

1. The sintering of Cu-20Zn prepared from prealloyed powder occurs along with liquid-phase formation and is of supersolidus type.
2. Changes in physical and mechanical properties with rising sintering temperature agree well with each other, and the results of microstructural and fractographic analysis confirm them. Based on the above mentioned changes, the optimum sintering temperature is approximately 930 °C.
3. An increase in sintering temperature results in decrease of pore number and causes sphericity as well as significant grain growth. Moreover, at lower sintering temperatures (<930 °C), the capillary force is the dominant factor and induces quick densification.
4. According to fractographic images, at lower sintering temperatures, the fracture occurs in regions containing solidified melt (grain boundary regions), but increasing sintering temperature results in densification and so the fracture occurs in transgranular and intergranular regions.
5. According to fractographic investigation and microstructural analysis it can be concluded that low sintering temperatures due to insufficient interparticle bonding and high sintering temperatures because of excess liquid phase formation are not favorable. There is an optimum temperature which can contribute to achieving improved physical and mechanical properties.

ACKNOWLEDGMENT

The authors wish to express their sincere gratitude and appreciation to Mr. Tabatabai, the respected manager of Tabriz Powder Metallurgy Company, and Mr. Mahdioun, who is responsible for the internship projects of Sapco Company Tabriz branch, because of their financial assistance.

REFERENCES

1. Imai, H., Kosaka, Y., Kojima, A., Li, S., Kondoh, K., Umeda, J., Atsumi, H., “Characteristics and machinability of lead-free P/M Cu60–Zn40 brass alloys dispersed with graphite”, Powder Technol, 2010, 198, 417.
2. Katsuyoshi, K., Hisashi, I., Junko, U., Yoshiharu, K., Akimichi, K., “Environmental Benign Brass Alloys Dispersed With Graphite Particles Fabricated Via Solid-State Sintering Process”, Trans JWRI, Vol. 37, No. 2, 2008.
3. Avner, S. H., “Introduction to Physical Metallurgy”, 2 Ed., McGraw Hill, 1974, pp. 460-470.
4. Upadhyaya, G. S., “Sintered Metallic and Ceramic Materials”, John Wiley and Sons, LTD, 2000.
5. RadomyselSkii, I. D., Baglyuk, G. A., Mazharova, G. E., “Production and Properties of Brass-Base P/M Constructional Materials”, Powder Metall Met Ceram, 1986, 23, 218.
6. German, R. M., “Supersolidus Liquid Phase Sintering, Part I: Process Review”, Int J Powder Metall, 1990, 26, 23.
7. German, R. M., “Supersolidus Liquid Phase Sintering, Part II: Densification Theory”, Int J Powder Metall, 1990, 26, 35.
8. German, R. M., “Liquid Phase Sintering”, Published in English by Plenum Press, New York, NY, 1985.
9. German, R. M., “Supersolidus Liquid-Phase Sintering of Prealloyed Powders”, Metall Mater Trans A, 1997, 28A, 1553.
10. Momeni, H., Razavi, H., Shabestari, S., “Effect

of Supersolidus Liquid Phase Sintering on the Microstructure and Densification of the Al-Cu-Mg Prealloyed Powder", Iranian J Mater Sci Eng, 2011, 8, 10.
11. Sabahi Namini, A., Azadbeh, M., Mohammadzadeh, A., "Microstructure and Densification Behavior of Liquid Phase Sintered Cu-28Zn Prealloyed Powder", Sci Sinter, 2013, 45, 351.
12. Azadbeh, M., Danninger, H., Gierl-Mayer, C., "Particle rearrangement during liquid phase sintering of Cu-20Zn and Cu-10Sn-10Pb prepared from prealloyed powder", Powder Metall, 2013, 56, 342.
13. Mohammadzadeh, A., Azadbeh, M., Sabahi Namini, A., Densification and Volumetric Change During Supersolidus Liquid Phase Sintering of Prealloyed Brass Cu28Zn Powder: Modeling and Optimization, Sci Sinter, 2014, 46, 23.
14. German, R. M., Olevsky, E. A., "Modeling Grain Growth Dependence on the Liquid Content in Liquid-Phase-Sintered Materials", Metall Mater Trans A, 1998, 29A, 3057.
15. Liu, J., Lal, A., German, R. M., "Densification and Shape Retention in Supersolidus Liquid Phase Sintering", Acta Mater, 1999, 47, 4615.
16. Marchi, C. S., Felberbaum, L., Mortensen, A., "The Effect of Gravity on Solution-Reprecipitation during Liquid Phase Sintering', Metall Mater Trans A, 2000, 31A, 397.
17. Olevsky, E. A., German, R. M., Upadhyaya, A., "Effect of Gravity on Dimensional Change during Sintering- II: Shape Distortion", Acta Mater, 2000, 48, 1167.
18. Metals Handbook, "Heat Treating", Vol. 4, 10th Edition, ASM, Metals Park OH, 1990.